Intermediate asymptotics in nonlinear optical systems

Sonia Boscolo* and Sergei K. Turitsyn

Photonics Research Group, School of Engineering and Applied Science, Aston University, Birmingham B4 7ET, United Kingdom

(Received 5 September 2011; published 9 April 2012)

Using a fiber laser system as a specific illustrative example, we introduce the concept of intermediate asymptotic states in finite nonlinear optical systems. We show that intermediate asymptotics of nonlinear equations (e.g., coherent structures with a finite lifetime or distance) can be used in applications similar to those of truly stable asymptotic solutions, such as, e.g., solitons and dissipative nonlinear waves. Applying this general idea to a particular, albeit practically important, physical system, we demonstrate a novel type of nonlinear pulse-shaping regime in a mode-locked fiber laser leading to the generation of linearly chirped pulses with a triangular distribution of the intensity.

DOI: 10.1103/PhysRevA.85.043811 PACS number(s): 42.65.Sf, 42.55.Wd, 42.65.Re, 42.81.Dp

I. INTRODUCTION

Nowadays it is widely recognized that stable asymptotic solutions of nonlinear equations play an important role in physics, biology, and many other fields of science. Asymptotic solutions define the long-term evolution of a nonlinear system. Often, coherent asymptotic structures can be generated from rather arbitrary or easily satisfied initial conditions. Such asymptotic solutions can be featured rather differently. For instance, the well-known solitons are static solutions of a nonlinear wave equation [1], dispersion-managed solitons are periodic breathing-like (nonlinear Bloch wave) solutions [2], and the more recently observed similaritons are self-similarly evolving, parabolic-shaped solitary-wave solutions to the nonlinear Schrödinger (NLS) equation with gain in the quasiclassical limit [3]. Due to their stability, asymptotic solutions of nonlinear systems are used in a wide range of practical applications. In particular, an important area of application of nonlinear solitary waves is in mode-locked lasers, where the generation of stable single optical pulses with certain properties quite often is the key purpose of the laser system operation. In this paper, we consider this particular, but important example of a nonlinear optical system for illustration of a more general idea. The proposed idea is based on a rather simple observation. In many practical nonlinear systems, the evolution of a wave field in time or distance is finite. Accordingly, under certain conditions, even formally unstable structures with a finite lifetime or distance can be used for a variety of applications in such systems. The key condition is that the *intermediate asymptotics* field should leave the system (in the laser context, it should be outcoupled) before it becomes unstable. Such an approach based on intermediate asymptotic states discloses a range of new opportunities for nonlinear systems.

II. INTERMEDIATE ASYMPTOTIC DYNAMICS IN THE NLS EQUATION

First, we highlight how the intermediate asymptotics approach can provide new outlook even in rather well-studied systems by considering the very well-known integrable NLS equation [1], which is a fundamental equation of nonlinear science and, in particular, the key model governing the localized optical pulse propagation in an optical fiber [4]:

$$u_\xi = -i\tfrac{1}{2}u_{\tau\tau} + i|u|^2u. \tag{1}$$

Here, we use the dimensionless quantities: $u(\xi,\tau) = NU$, $U(\xi,\tau) = \psi/\sqrt{P_0}$, $\xi = z/L_D$, and $\tau = t/T_0$, where $\psi(z,t)$ is the slowly varying amplitude of the pulse envelope in a comoving frame, T_0 and P_0 are, respectively, some temporal characteristic value and the peak power of the initial pulse, and L_D, L_{NL}, and N are, respectively, the dispersion length, the nonlinear length, and the energy parameter ("soliton" number), defined as $L_D = T_0^2/|\beta^{(2)}|$, $L_{NL} = 1/(\gamma P_0)$, and $N = \sqrt{L_D/L_{NL}}$, where $\beta^{(2)}$ and γ are the respective group-velocity dispersion (GVD) and Kerr nonlinearity parameters of the fiber. In the normal-dispersion regime of the fiber, starting from an arbitrary bell-shaped initial field distribution, e.g., from a Gaussian pulse, it is possible to generate some advanced field distributions, such as parabolic-, flat-top-, and triangular-profiled pulses with a linear frequency chirp [5]. Such pulse waveforms represent transient states of the nonlinear pulse evolution in the fiber medium and can be associated with an intermediate asymptotic regime of the pulse propagation. Intermediate asymptotic evolution is of crucial importance in nonlinear physics, as it describes the development of a self-similar system at propagation distances such that the fine structure due to the boundaries has disappeared yet the system has not reached its asymptotic state [6]. For the triangular pulse state being considered in this paper, this corresponds to the fact that a self-similar nature of the propagation is dominant over some finite distance so that we can identify a triangular pulse, yet the asymptotic pulse solution has not been reached. The characteristic length scale of the self-similar triangular pulse dynamics, or life distance, depends on the initial pulse features (shape, energy, and chirp profile).

Different approaches are possible to characterize the pulse shape [5,7]. Here we choose the parameter of misfit M_S between the pulse temporal intensity profile and a specific shape fit $|u_S(\tau)|^2$ of the same energy and full width at half-maximum (FWHM) duration: $M_S^2 = \int d\tau\,(|u|^2 - |u_S|^2)^2/\int d\tau\,|u|^4$. An example of the evolution of an initial Gaussian pulse toward a pulse with a

*s.a.boscolo@aston.ac.uk

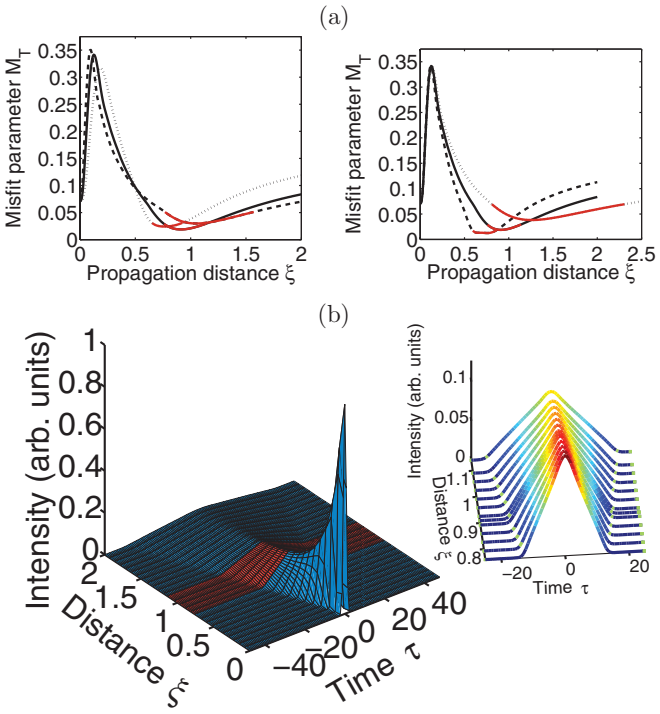

FIG. 1. (Color online) Evolution of an initial Gaussian pulse in the fiber. (a) Evolution of the misfit parameter to a triangular temporal shape for varying values of N and the (normalized) chirp parameter C. Left: $N = 6$ (dotted curve), $N = 10$ (solid curve), and $N = 14$ (dashed curve); $C = 1$. Right: $C = 0.75$ (dotted curve), $C = 1$ (solid curve), and $C = 1.25$ (dashed curve); $N = 10$. Gray (red) lines define the life distances of the triangular pulses. (b) Evolution of the intensity profile for $N = 10$ and $C = 1$. The profiles at distances $\xi_0 \leqslant \xi \leqslant \xi_0 + \xi_{\text{life}}$ are drawn in red and shown in the inset.

triangular intensity profile is presented in Fig. 1. We define here the life distance ξ_{life} of the triangular solution as the distance in the fiber where the misfit parameter to a triangular shape $M_T \leqslant M_T(\xi_*)$, where ξ_* is the closest position to the point of absolute minimum of the M_T curve where the gradient of the curve $|dM_T/d\xi|$ becomes equal to or greater than a sufficiently small value, which is set to 0.15 as an example. Both the distance where M_T reaches a minimum and the life distance of the triangular solution increase for increasing values of N, showing that formation of a triangular-shaped pulse happens later in propagation distance and this pulse form is maintained over larger distances. Larger values of the initial chirp parameter lead to an earlier onset of the triangular pulse evolution and a better fit of the triangular profile, whereas the formed shape is maintained over shorter distances. We note that a necessary condition for triangular pulse formation in the fiber is that the initial pulse has a nonzero, positive chirp (using the definition $iC\tau^2$ for the phase profile) [5]. We note also that for a different choice of the initial pulse shape, similar pulse-shaping regimes occur upon propagation in the fiber, whereas the relevant parameter regions are different. We find that in the quasiclassical or WKB limit of Eq. (1) (i.e., the limit of high amplitude or small dispersion such that $|(|u|)_{\tau\tau}|/(2|u|^3) \ll 1$), the dynamic evolution

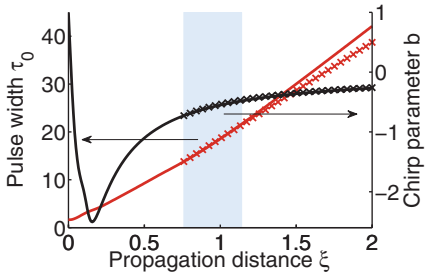

FIG. 2. (Color online) Evolution of the pulse width $\tau_0(\xi)$ [gray (red) line] and chirp parameter $b(\xi)$ (black line) for $N = 10$ and $C = 1$: solid curves, simulation results; crosses, theoretical predictions from (2b) and (2c) for $\xi \geqslant \xi_0$. The shaded region defines the life distance of the triangular solution.

of the formed triangular pulse can be modeled as $u(\xi,\tau) = \sqrt{p_0(\xi)}[1 - |\tau/\tau_0(\xi)|]^{1/2} \exp[ib(\xi)\tau^2 + i\phi_0(\xi)]\theta(\tau_0(\xi) - |\tau|)$, where $\theta(x)$ is the Heaviside function, and the peak power $p_0(\xi)$, pulse width $\tau_0(\xi)$, and chirp parameter $b(\xi)$ are given by

$$p_0(\xi) = \frac{p_0(\xi_0)}{1 - 2b(\xi_0)(\xi - \xi_0)}, \tag{2a}$$

$$\tau_0(\xi) = \tau_0(\xi_0)[1 - 2b(\xi_0)(\xi - \xi_0)], \tag{2b}$$

$$b(\xi) = \frac{b(\xi_0)}{1 - 2b(\xi_0)(\xi - \xi_0)}. \tag{2c}$$

Here, ξ_0 is the initial transition distance preceding the triangular regime, and Eqs. (2a) and (2b) give the energy-conservation condition. Figure 2 shows an example of the evolution of the pulse parameters obtained from fits to the propagating pulse from simulations. The expected results obtained from Eqs. (2b) and (2c) calculated for $\xi \geqslant \xi_0$ are in good agreement with the simulation values, even at propagation distances $\xi > \xi_0 + \xi_{\text{life}}$.

III. NONLINEAR PULSE SHAPING IN MODE-LOCKED FIBER LASERS

Next, we demonstrate how intermediate asymptotics can be exploited in a practical laser system. Rapid recent progress in passively mode-locked fiber lasers is closely linked to new nonlinear regimes of pulse generation, namely, the self-similar parabolic pulse [8] and the all-normal-dispersion (dissipative soliton) [9] regimes. These are fundamentally different from the well-known soliton [10] and dispersion-managed soliton [11] regimes. In 2010 Oktem and colleagues [12] demonstrated an entirely new regime of mode locking in a fiber laser simultaneously sustaining distinctly different amplifier similariton and soliton pulses. Amplifier similaritons were also demonstrated in an all-normal dispersion fiber laser [13] and in a Raman fiber laser [14]. Mode-locked fiber lasers are complex physical systems exhibiting a nontrivial interplay among the effects of gain, dispersion, and nonlinearity. This interplay can be used to shape the pulses and pulse dynamics and, hence, lead to different mode-locking regimes. This makes such lasers interesting realizations of so-called

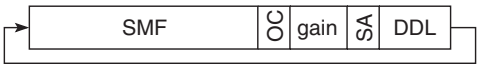

FIG. 3. Schematic model for the laser. SMF, single-mode fiber; OC, output coupler; SA, saturable absorber; DDL, dispersive delay line.

dissipative nonlinear systems [15] with a variety of possible pulse-shaping mechanisms not yet fully explored. Here we report numerical predictions of the existence of two distinct steady-state solutions of stable single pulses in a laser cavity in different regions of the system parameter space: the previously known self-similar parabolic pulse and a pulse with a triangular temporal profile and a linear frequency chirp. To the best of our knowledge, this is the first report of the possibility of triangular pulse shaping in mode-locked lasers.

In our modeling, to stress the generality of the results, we use a rather standard laser cavity similar to that described in Ref. [8] as an example (Fig. 3). A 6-m-long segment of single-mode fiber (SMF) with normal GVD forms the major part of the cavity and is connected to a short length—0.3 m—of ytterbium-doped gain fiber that provides pulse amplification. An output coupler (OC) is placed at the end of the SMF where interesting pulse shapes are observed. The gain fiber is followed by a saturable absorber element. The final element is a dispersive delay line (DDL) that provides anomalous GVD with negligible nonlinearity. The cavity is a ring, and thus, after the DDL the pulse returns to the SMF. Numerical simulations are based on a modified NLS equation, expressed in a dimensional form as

$$\psi_z = -i\frac{\beta^{(2)}}{2}\psi_{tt} + i\gamma|\psi|^2\psi + \frac{1}{2}g * \psi. \tag{3}$$

Here, $\beta^{(2)} = 25\ \mathrm{fs}^2/\mathrm{mm}$, $\gamma = 0.005\ (\mathrm{W\,m})^{-1}$, $*$ represents the Fourier convolution, and $g(t)$ is the inverse Fourier transform of the gain spectrum given by

$$g = \frac{g_0}{1 + W/W_{0,g} + (\omega-\omega_0)^2/\Omega_g^2} \approx \frac{g_0}{1+W/W_{0,g}}\left[1-(\omega-\omega_0)^2/\Omega_g^2\right], \tag{4}$$

where g_0 is the small-signal gain, which is nonzero only for the gain fiber, ω_0 is the central angular frequency, Ω_g is the gain bandwidth, which is chosen to correspond to a 40-nm FWHM bandwidth, $W(z) = \int dt\,|\psi|^2$ is the pulse energy, and $W_{0,g} = 400$ pJ is an effective gain saturation energy corresponding to the saturation power (determined by the pump power) for a given repetition rate. The OC is described by a coupling coefficient R such that at each round-trip the fraction of input field that passes through is given by $\psi_{\mathrm{pass}}(t)/\psi_{\mathrm{in}}(t) = \sqrt{R}$. The linear losses inside the cavity are accounted for by R without loss of generality. The saturable absorber is modeled by a transfer function that describes its transmittance $T(t) = 1 - q_0/[1 + P(t)/P_{0,a}]$, where $q_0 = 0.3$ is the unsaturated loss, $P(z,t) = |\psi(z,t)|^2$ is the instantaneous pulse power, and $P_{0,a} = 150$ W is the saturation power.

Two practically tunable system parameters, namely, the net cavity dispersion $\beta^{(2)}_{\mathrm{net}}$ and the integrated gain of the gain fiber G, are varied to achieve different mode-locking

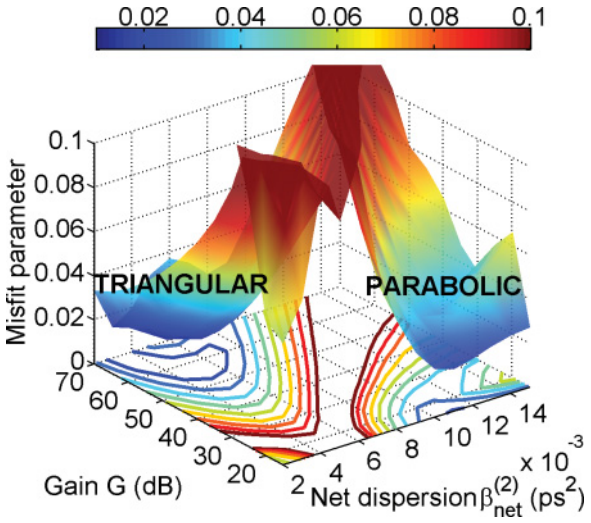

FIG. 4. (Color online) Misfit parameters of the steady-state pulses to parabolic and triangular temporal shapes at the end of the SMF versus net cavity dispersion and total gain. Misfit values >0.1 are rendered with the same color associated with 0.1. The coupling coefficient $R = 0.1$.

regimes. Here $\beta^{(2)}_{\mathrm{net}}$ is varied by changing the dispersion compensation provided by the DDL, and G is varied by changing the small-signal gain g_0. A Gaussian pulse with the energy 66 pJ and the FWHM duration 0.1665 ps is used as the initial condition at the input of the SMF. Results of the characterization of the steady-state pulse shapes at the end of the SMF section for the laser operating at normal net dispersion and with $R = 0.1$ are shown in Fig. 4. We can see that pulses with a parabolic temporal shape are obtained for relatively large values of the net dispersion and moderate gain values. In contrast, triangular-shaped pulses are observed for smaller net dispersion and rather high gain values. We note that the formation of better-quality triangular pulses at the SMF output for realistic gain values from 20 to 40 dB is possible by use of an SMF with higher nonlinearity. Furthermore, at such gains close-to-ideal triangular shapes generally form earlier in propagation distance within the SMF. Then placing a small OC about such a position in the SMF would permit extraction of the sought pulses from the cavity. This would effectively correspond to extracting the intermediate asymptotics field from the cavity before it becomes unstable.

Solutions obtained at representative points in the parameter space of the parabolic and triangular pulse regimes are shown in Fig. 5. The pulse evolution is illustrated by plots of the root-mean-square (rms) pulse duration, spectral bandwidth, and chirp parameter as functions of position in the cavity (Fig. 6). For the parabolic pulse regime, the parabolic temporal profile after the SMF, linear frequency chirp, and imaging of the temporal shape in the spectral domain are all signatures of what is well known from self-similar propagation and mode locking [3,8] and are due to self-similar evolution in the SMF. The nonlinear evolution in the SMF is monotonic with the growth of both temporal and spectral widths. The generated bandwidth is filtered by the gain medium, and the pulse is always negatively chirped inside the cavity with a minimum just after entering

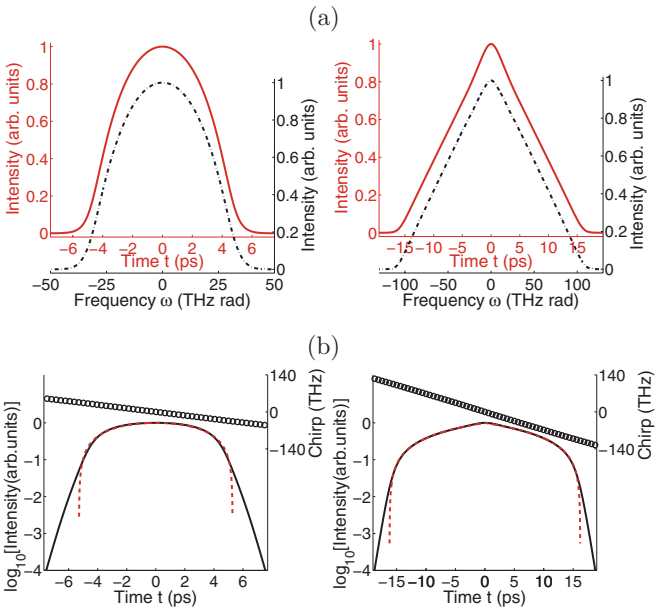

FIG. 5. (Color online) (a) Temporal [solid (red) curves] and spectral [dash-dotted (black) curves] profiles of the pulse at the end of the SMF for $\beta_{\text{net}}^{(2)} = 0.011$ ps^2 and $G = 20$ dB (left) and for $\beta_{\text{net}}^{(2)} = 0.004$ ps^2 and $G = 60$ dB (right). (b) Temporal intensity profiles on a log scale [solid (black) curves] and chirp profiles [open (black) circles]. Dashed (red) curves: parabolic (left) and triangular (right) fits. The coupling coefficient $R = 0.1$.

the SMF [8]. In the case of triangular pulse shaping, pulses with both triangular temporal and spectral intensity profiles are obtained after the SMF. The spectral shape reflecting the temporal shape is again a result of the linear chirp and high value of the chirp coefficient. This can be explained using the stationary phase method, i.e., the cancellation of oscillating contributions with rapidly varying phase. Consider the linearly chirped pulse, $\psi_S(t) = A(t)\exp(ibt^2 + \phi_0)$, where $|\psi_S(t)|^2$ is a parabolic (S = P) or triangular (S = T) fit to the actual pulse shape $|\psi(t)|^2$, and b is the chirp coefficient. The points of

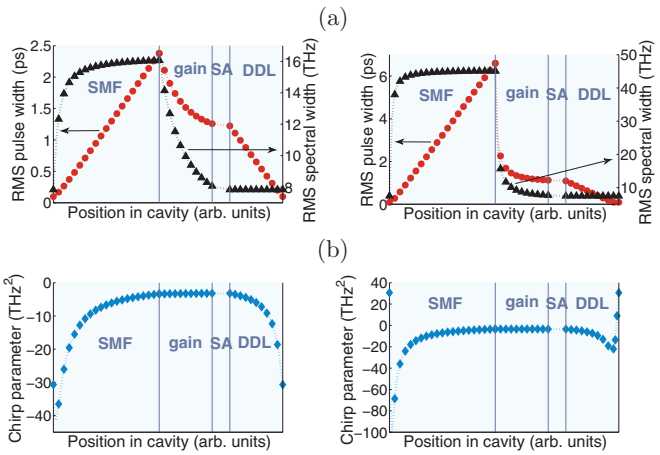

FIG. 6. (Color online) Evolution of (a) the rms temporal [(red) circles] and spectral [(black) triangles] widths and (b) the chirp parameter [(blue) diamonds] along the cavity for $\beta_{\text{net}}^{(2)} = 0.011$ ps^2 and $G = 20$ dB (left) and for $\beta_{\text{net}}^{(2)} = 0.004$ ps^2 and $G = 60$ dB (right). The coupling coefficient $R = 0.1$.

stationary phase in $\psi_S(t)\exp(i\omega t)$ are the times $t_0 = -\omega/(2b)$. Approximating the phase with a Taylor series expansion about the dominant time t_0 and neglecting terms of order higher than $(t - t_0)^2$, it can be seen that when b is relatively large, even a small difference $(t - t_0)$ generates rapid oscillations within the Fourier transform integral, leading to cancellation of such terms. In other words, the limits of integration are extended beyond the limit for a Taylor expansion, which yields a parabolic or triangular spectral shape for $\psi_S(t)$. Similarly to the parabolic pulse regime, the nonlinear evolution in the SMF is monotonic, though the scales of temporal and spectral broadening are larger. The main difference from the parabolic regime is that the chirp is changed from negative at the end of the gain fiber to positive at the entrance of the SMF by the DDL, and correspondingly, the pulse compresses to minimum duration in the DDL. We note that the positive sign of the chirp coefficient at the entrance of the SMF is consistent with our previously reported findings on triangular pulse generation in one-stage fiber systems [5,16].

The triangular pulse intermediate asymptotic dynamics has been investigated using additional propagation in the SMF at the laser output. We have observed that larger integrated cavity gain and larger net cavity dispersion both generally lead to the formation of triangular pulses later in propagation distance and to a larger life distance of the formed pulses. In particular, this means that at a large gain or dispersion the outcoupled intermediate asymptotics field can still propagate over some distance before becoming unstable. A detailed study will be presented in future work. We have also analyzed the dependence of the pulse-shaping regimes on the energy coupled inside and outside the cavity, with results showing that in the range of net cavity dispersions and gains explored, in contrast to the parabolic regime, the triangular regime appears to be almost independent of the energy coupling, thus offering more flexibility in the laser design.

IV. CONCLUSION

Using intermediate asymptotics in finite nonlinear optical systems, we have proposed to produce field distributions that cannot be created using asymptotically stable solutions. Taking into account the finite nature of the spatial and temporal scales related to physical systems, the possibility of generating nonlinear pulse waveforms that reproduce themselves on some distance could be of great interest for many practical applications in nonlinear optics. We have demonstrated the possibility of pulse shaping in a mode-locked fiber laser using control of the intracavity propagation dynamics by adjustment of the normal net dispersion and integrated gain. The existence of a novel type of pulse shaping regime that produces pulses with a triangular temporal intensity profile and a linear frequency chirp has been shown. From a fundamental viewpoint, these results are interesting from the perspective of the physics of dissipative nonlinear systems. From a practical viewpoint, the simple intensity profile of triangular pulses is attractive for various photonic applications, including time-domain add-drop multiplexing, wavelength conversion [17], and doubling of optical pulses in the frequency and time domains [18].

[1] V. E. Zakharov and A. B. Shabat, Zh. Eksp. Teor. Fiz. **61**, 118 (1971) [Sov. Phys. JETP **34**, 62 (1972)].
[2] I. Gabitov and S. K. Turitsyn, Opt. Lett. **21**, 327 (1996).
[3] M. E. Fermann, V. I. Kruglov, B. C. Thomsen, J. M. Dudley, and J. D. Harvey, Phys. Rev. Lett. **84**, 6010 (2000).
[4] G. P. Agrawal, *Nonlinear Fiber Optics*, 4th ed. (Academic Press, San Diego, CA, 2006).
[5] S. Boscolo, A. I. Latkin, and S. K. Turitsyn, IEEE J. Quantum Electron. **44**, 1196 (2008).
[6] G. I. Barenblatt, *Scaling, Self-Similarity, and Intermediate Asymptotics* (Cambridge University Press, Cambridge, 1996).
[7] A. Ruehl, O. Prochnow, D. Wandt, D. Kracht, B. Burgoyne, N. Godbout, and S. Lacroix, Opt. Lett. **31**, 2734 (2006).
[8] F. Ö. Ilday, J. R. Buckley, W. G. Clark, and F. W. Wise, Phys. Rev. Lett. **92**, 213902 (2004).
[9] A. Chong, J. Buckley, W. Renninger, and F. Wise, Opt. Express **14**, 10095 (2006).
[10] I. N. Dulin III, Electron. Lett. **27**, 544 (1991).
[11] K. Tamura, E. P. Ippen, and H. A. Haus, Appl. Phys. Lett. **67**, 158 (1995).
[12] B. Oktem, C. Ülgüdür, and F. Ö. Ilday, Nat. Photon. **4**, 307 (2010).
[13] W. H. Renninger, A. Chong, and F. W. Wise, Phys. Rev. A **82**, 021805 (2010).
[14] C. Aguergaray, D. M'echin, V. Kruglov, and J. D. Harvey, Opt. Express **18**, 8680 (2010).
[15] N. Akhmediev and A. Ankiewicz (eds.), *Dissipative Solitons, Lecture Notes in Physics,* Vol. 661 (Springer, Berlin, 2005).
[16] H. Wang, A. I. Latkin, S. Boscolo, P. Harper, and S. K. Turitsyn, J. Opt. **12**, 035205 (2010).
[17] F. Parmigiani, M. Ibsen, P. Petropoulos, and D. J. Richardson, IEEE Photonics Technol. Lett. **21**, 1837 (2009).
[18] A. I. Latkin, S. Boscolo, R. S. Bhamber, and S. K. Turitsyn, J. Opt. Soc. Am. B **26**, 1492 (2009).